ISSN 0036-0295, Russian Metallurgy (Metally), Vol. 2021, No. 9, pp. 1085–1092. © Pleiades Publishing, Ltd., 2021.
Russian Text © The Author(s), 2021, published in Metally, 2021, No. 5, pp. 50–58.

Effect of Equal-Channel Angular Pressing on the Structure, Mechanical Characteristics, and Aging Behavior of Cu–7% Cr and Cu–10% Fe Alloys

N. S. Martynenko[a, *], N. R. Bochvar[a], P. B. Straumal[a], D. A. Aksenov[b, c], G. I. Raab[c], and S. V. Dobatkin[a, d]

[a] *Baikov Institute of Metallurgy and Materials Science, Russian Academy of Sciences, Moscow, Russia*
[b] *Institute of Molecule and Crystal Physics, Ufa Federal Research Center, Russian Academy of Sciences, Ufa, Russia*
[c] *Ufa State Aviation Technical University, Ufa, Russia*
[d] *National University of Science and Technology MISiS, Moscow, Russia*
**e-mail: nmartynenko@imet.ac.ru*

Received March 24, 2021; revised April 20, 2021; accepted May 13, 2021

Abstract—The effect of equal-channel angular pressing (ECAP) and subsequent aging on the structure and mechanical properties of Cu–7% Cr and Cu–10% Fe alloys is studied. ECAP is shown to substantially refine the structure of both alloys. The average grain and subgrain sizes of the Cu–7% Cr and Cu–10% Fe alloys subjected to ECAP are 250 ± 13 and 155 ± 7 nm, respectively. Moreover, the presence of shear bands ~100 nm wide is found for the alloys. The structure refinement results in a substantial increase in the strength of the alloys and a simultaneous decrease in their plasticity. In this case, additional aging of the alloys, which is performed after quenching, increases their microhardness, electrical conductivity, and strength; simultaneously, the plasticity decreases. Aging of the alloys subjected to ECAP leads to an increase in the sizes of the structural components (both shear bands and grains and subgrains) and to the precipitation of chromium and iron phases from the Cu–7% Cr and Cu–10% Fe alloys, respectively. The average sizes of shear bands, grains, and subgrains of the Cu–7% Cr and Cu–10% Fe alloys subjected to ECAP and aging are 130 ± 7 and 317 ± 24 nm and 220 ± 9 and 357 ± 27 nm, respectively. Aging does not affect the strength of the deformed Cu–7% Cr alloy and leads to a softening of the deformed Cu–10% Fe alloy. Aging of both alloys subjected to ECAP leads to an increase in their plasticity and electrical conductivity. In the case of the Cu–7% Cr alloy, treatment, which consists in quenching, ECAP, and aging, ensures reaching a better combination of the strength (~470 MPa), plasticity (~18%), and electrical conductivity (~81% IACS).

Keywords: copper alloys, equal-channel angular pressing, aging, microstructure, mechanical characteristics, electrical conductivity

DOI: 10.1134/S003602952109010X

INTRODUCTION

Equal-channel angular pressing (ECAP) intended for improving the mechanical and functional properties of metallic materials has been widely used in practice for a long time [1–4]. Owing to the creation of conditions for high shear deformation, a microstructure can be substantially refined up to ultrafine-grained (UFG) and nanostructured states. The formation of such structures leads to an increase in the strength and the improvement of many service properties. In particular, the application of ECAP for magnesium alloys allows one to increase their corrosion resistance [5]; in the case of steels, an increase in the fatigue life is observed [6]. At the same time, ECAP and subsequent aging of quenched aluminum and copper alloys ensure a combination of a high strength and electrical conductivity of these materials; this is of particular importance for their application in the electrical industry [7–10].

Among the most popular materials for the electrical industry, copper alloys are distinguished [11, 12]. They are widely used in manufacturing resistance-welding electrodes, wire, and carrier cables. For such an application, not only a good strength of matrix material but also its high thermal stability, i.e., the fact that the material retains the strength at high temperatures, is of importance. Because of this, the development and study of new compositions is a challenging problem. At present, Cu–Cr alloys, in particular, low-alloyed chromium bronzes are most widely used as materials for electric purposes [13, 14]. These materials are used mainly due to their relatively low cost. However, the thermal stability of deformed low-alloyed bronzes (to 200–300°C) is insufficient to use

them in critical constructions [15]. The mechanical characteristics of these alloys can be improved by increasing the chromium content in their composition. Earlier, high-chromium copper alloys already were studied [16–18]. Moreover, the Cu–Fe system [19–22], in particular, a Cu–10% Fe alloy [20, 21], shows promise as materials for electric application. However, it is necessary to note that the strength of copper alloys is not high. Because of this, it is reasonable to study the effect of severe plastic deformation (SPD) on the mechanical behavior of Cu–Cr and Cu–Fe alloys with a high content of alloying elements.

The purpose of this work is to study the effect of ECAP on the structure, mechanical characteristics, and aging behavior of the Cu–7% Cr and Cu–10% Fe alloys, which show promise for the application in electrical industry.

EXPERIMENTAL

Ingots of Cu–7% Cr and Cu–10% Fe alloys were prepared by vacuum arc melting. Cast blanks 100 mm in diameter were used to form rods 10 mm in diameter by hot forging at 800°C. Before ECAP, blanks of both alloys were subjected to homogenizing annealing at 1000°C for 2 h and subsequent water quenching. ECAP was performed at room temperature in accordance with route B_c using a die having a 90° channel intersection. For both alloys, the total number of passes was $n = 4$.

The microstructure of the quenched alloys was studied using an Axio Observer D1m optical microscope (Carl Zeiss). After ECAP, the microstructure of alloys was studied on a Jeol JEM 2100 electron microscope operating at an accelerating voltage of 200 kV. To prepare foils, samples preliminarily were thinned on an abrasive paper and subjected to polishing using a TENUPOL 5 polisher. To calculate the size of structural components, a random secant method was used. The calculations were performed using the Image Expert Pro 3 software.

The supersaturated solid-solution decomposition processes that occur in the alloys upon aging were studied via plotting the dependences of the microhardness and electrical conductivity on the aging temperature t ($\tau = 1$ h) and time ($T = $ const). The microhardness of the alloys was studied using a 402 MVD Instron Wolpert Wilson Instruments tester and the 1 N (100 gf) load; the exposition time is 10 s. The electrical conductivity of the alloys was studied via the measuring the electrical resistivity using plain samples (1.5 × 4.5 × 10 mm in size) and a BSZ-010-2 microhmmeter. After that, the values of electrical resistivity were recalculated into the specific electrical conductivity and transformed into percentage ratio to that of annealed copper in accordance with the International Annealed Copper Standard (% IACS).

The mechanical properties were studied by uniaxial tension at room temperature on an Instron 3382 testing machine using plain samples 2 × 1 mm in gage section and 5.75 mm in gage length at a strain rate of 1 mm/min.

RESULTS AND DISCUSSION

Figure 1 shows the microstructure of the Cu–7% Cr and Cu–10% Fe alloys in the initial quenched state and after ECAP. The structure of both alloys in the quenched state consists of coarse grains of copper-based supersaturated solid solution 30–35 μm in size. In this case, second phase particles 3–5 μm in size are present in the microstructure of the alloys. Such particles in the Cu–7% Cr and Cu–10% Fe alloys correspond to the chromium (Fig. 1a) and iron (Fig. 1b) phase, respectively [23]. It should be noted that annealing twins 3–5 μm in size are present in the structure of both the quenched alloys.

ECAP of both alloys leads to the formation of a mixed UFG structure, which consists of shear bands and a grain–subgrain structure. In the Cu–7% Cr alloy subjected to ECAP, shear bands ~100 nm wide and grains and subgrains with an average size of 250 ± 13 nm are observed (Figs. 1c, 1e). In the Cu–10% Fe alloy subjected to ECAP, the presence of shear bands ~100 nm wide along with grains and subgrains with an average size of 155 ± 7 nm is noted (Figs. 1d, 1f). It should be also noted that the formation of grains and subgrains take place both outside and inside shear bands.

Both alloys under study are among the precipitation-hardening materials, the heat treatment of which is accompanied by the decomposition of a supersaturated solid solution. In practice, this should lead to improvement of the strength and/or functional properties (in our case, such a property is electrical conductivity). Figures 2a and 2b show data on the microhardness and electrical conductivity of the Cu–7% Cr and Cu–10% Fe alloys in the quenched state and after ECAP in accordance with the aging temperature. First, it should be noted that ECAP of both alloys leads to an increase in the microhardness as a result of the grain refining. The microhardness of the Cu–7% Cr alloy increases from 1.11 ± 0.03 to 1.58 ± 0.06 GPa; in the case of the Cu–10% Fe alloy, the microhardness increases from 1.18 ± 0.06 to 1.69 ± 0.06 GPa. The study of the changes in the microhardness during aging showed that the microhardness of the Cu–7% Cr alloy was unchanged in a temperature range from 20 to 350°C. An increase in the microhardness is observed beginning from a temperature of 400°C. At 500°C, the microhardness decreases almost to the initial value. At the same time, the microhardness of the Cu–7% Cr alloy subjected to ECAP remains unchanged up to 425°C and, as the temperature increases, decreases abruptly (see Fig. 2a).

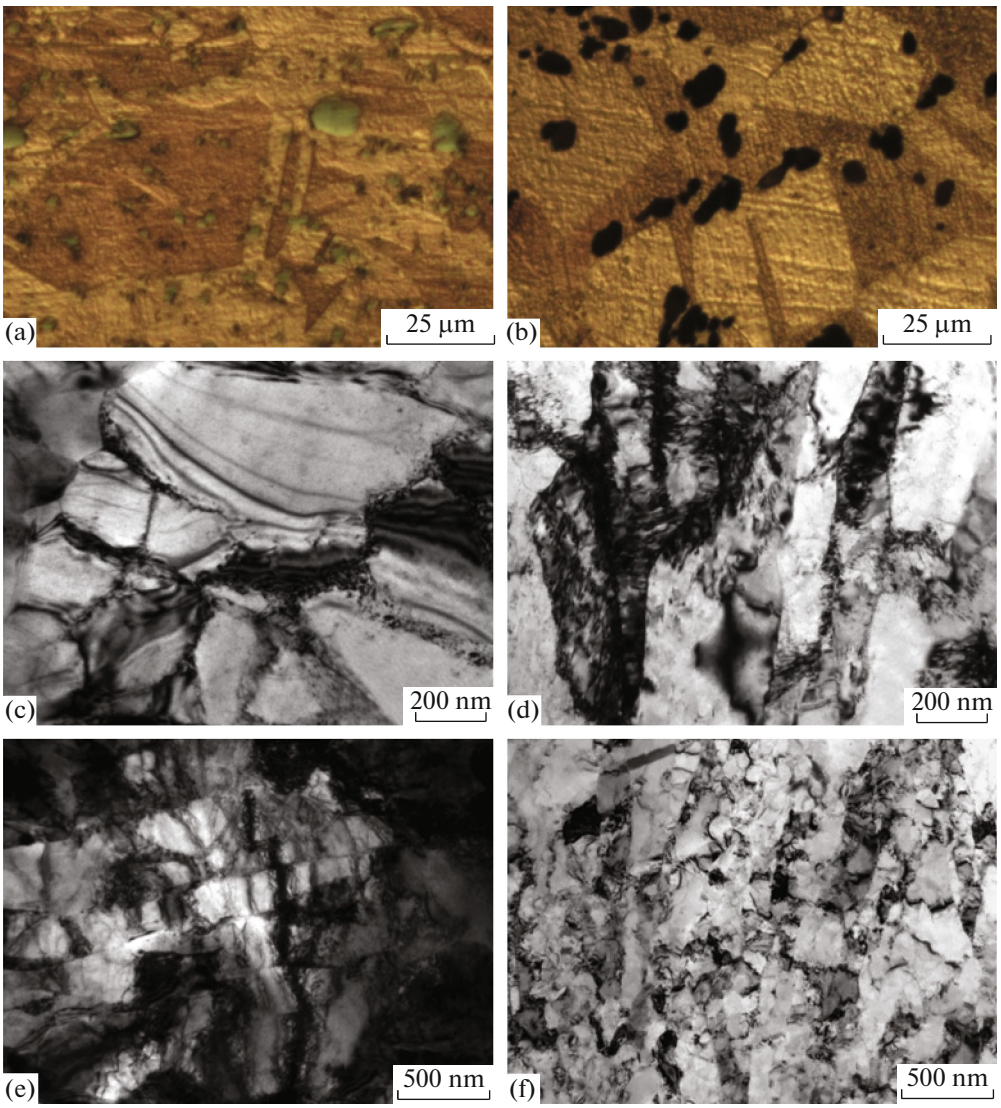

Fig. 1. Microstructure of (a, c, e) Cu–7% Cr and (b, d, f) Cu–10% Fe alloys in (a, b) quenched state and (c–f) after ECAP.

The decomposition of supersaturated solid solution in the Cu–10% Fe alloy in both the microstructural states has no the strengthening effect. The values of microhardness of the quenched alloy almost are the same within the whole aging temperature range, whereas the microhardness of the deformed alloy slightly decreases after aging at temperatures above 500°C (see Fig. 2a). Despite the data, the study of the electrical conductivity indicates the fact that the decomposition of the solid solution occurs in both alloys (Fig. 2b). An increase in the electrical conductivity of the Cu–7% Cr alloy in both microstructural states is observed after aging above 400°C and, therefore, indicates the active occurrence of the solid solution decomposition. In this case, the more intense increase in the microhardness of the deformed Cu–7% Cr alloy is likely to be caused by the presence of a great number of crystal lattice defects (dislocations) formed in the course of the ECAP. Dislocations act as particle crystallization centers; this accelerates the solid solution decomposition [24–26].

Despite the absence of strengthening during heating, the Cu–10% Fe alloy also exhibits the increase in the electrical conductivity at aging temperatures above 400°C. This confirms the particle precipitation upon decomposition and depletion of the supersaturated solid solution (see Fig. 2b).

Based on the data obtained, the isothermal annealing temperatures were chosen. The aging temperature of both the quenched alloys and the Cu–10% Fe alloy subjected to ECAP is 500°C, whereas the aging temperature of the deformed Cu–7% Cr alloy is 425°C.

Figures 2c and 2d show the dependences of the microhardness and electrical conductivity on the aging time. The quenched Cu–7% Cr alloy is seen to

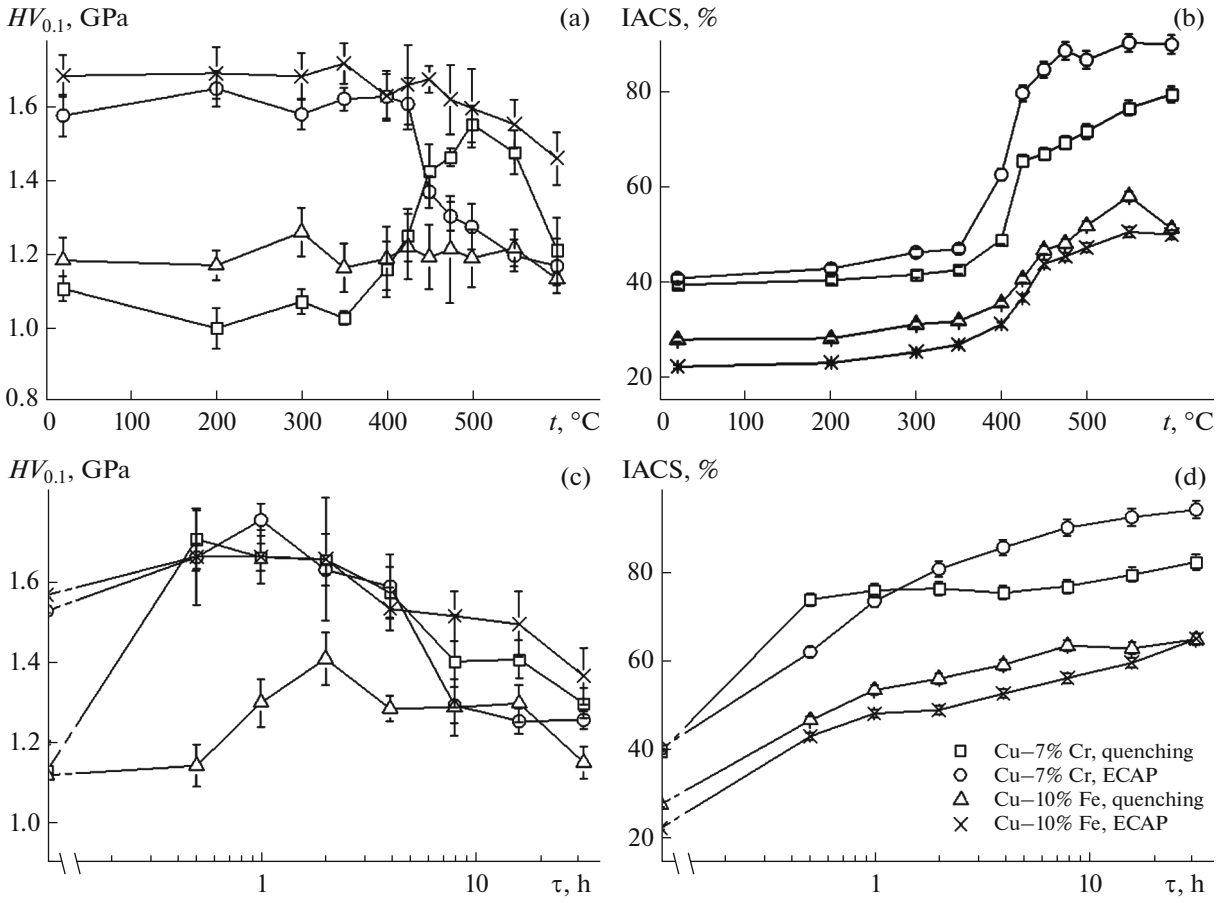

Fig. 2. Dependences of the (a, c) microhardness $HV_{0.1}$ and (b, d) electrical conductivity IACS of the Cu–7% Cr and Cu–10% Fe alloys before and after ECAP on the aging temperature and time.

undergo the most pronounced strengthening; the peak microhardness is reached after 30-min aging. In this case, the microhardness slightly changes within 4 h and, after that, decreases abruptly. At the same time, the microhardness of the ECAP-processed Cu–7% Cr alloy is almost unchanged for 4 h (only a slight increase corresponds to 1 h) and then abruptly decreases. In the case of the quenched Cu–10% Fe alloy, the peak microhardness corresponds to aging at 500°C for 2 h. However, it should be noted that this peak is not so pronounced as compared to that for the quenched Cu–7% Cr alloy. In this case, the microhardness of the deformed Cu–10% Fe alloy is unchanged for 2-h aging and then begins to decrease. The increase in the electrical conductivity of the alloys under study indicates the fact that, during aging, the supersaturated solid solution decomposition processes occur in the alloys in both the states (Fig. 2d). In this case, the solid solution decomposition in the Cu–7% Cr alloy is more pronounced (in particular, in deformed state) as compared to that in the Cu–10% Fe alloy.

Taking into account the results of the study of aging kinetics, aging parameters of the alloys were chosen, the application of which ensures reaching the optimum combinations of the microhardness and electrical conductivity. For both the quenched alloys and ECAP-processed Cu–10% Fe alloy, such a parameter was chosen to be heating at 500°C for 2 h; the aging of the ECAP-processed Cu–7% Cr alloy was performed at 425°C for 2 h. In the case of the use of the above conditions, the microhardness and electrical conductivity are sufficiently high. Table 1 gives the summarized data on aging of the Cu–7% Cr and Cu–10% Fe alloys.

Figure 3 shows the microstructures of the studied alloys subjected to ECAP and subsequent aging under the optimum conditions. The structure of the Cu–7% Cr alloy subjected to ECAP and aging is fragmented and mixed, i.e., shear bands and cellular microstructure are observed (Figs. 3a, 3b). Low-angle boundaries of fragments are formed by dislocation walls. In this case, the average lateral size of fragments is 130 ± 7 nm. Within the fragment body, developed dislocation networks are observed, at which fine chromium phase particles 5 nm in size and large particles 12 ± 1 nm in average size are pinned. Moreover, the presence of grain–subgrain structure with an average size of 317 ±

Table 1. Microhardness ($HV_{0.1}$) and electrical conductivity (IACS) of Cu–7% Cr and Cu–10% Fe alloys in different microstructural states

Alloy: treatment	$HV_{0.1}$, GPa	IACS, %
Cu–7%Cr: quenching	1.13 ± 0.07	39.7 ± 0.7
ECAP	1.53 ± 0.03	40.4 ± 0.7
quenching + aging at 500°C for 2 h	1.66 ± 0.06	76.6 ± 1.6
ECAP + aging at 425°C for 2 h	1.63 ± 0.01	81.0 ± 1.7
Cu–10%Fe: quenching	1.12 ± 0.09	27.8 ± 0.5
ECAP	1.57 ± 0.04	22.5 ± 0.4
quenching + aging at 500°C for 2 h	1.41 ± 0.07	56.2 ± 1.1
ECAP + aging at 500°C for 2 h	1.66 ± 0.16	49.1 ± 0.9

Table 2. Mechanical characteristics of Cu–7% Cr and Cu–10% Fe alloys in different microstructural states

Alloy: treatment	$\sigma_{0.2}$	σ_u	δ, %
	MPa		
Cu–7% Cr: quenching	140 ± 13	288 ± 6	48.0 ± 4.3
ECAP	465 ± 13	480 ± 6	14.8 ± 1.3
quenching + aging at 500°C for 2 h	356 ± 12	430 ± 27	21.2 ± 4.9
ECAP + aging at 425°C for 2 h	435 ± 18	472 ± 12	18.1 ± 3.6
Cu–10% Fe: quenching	238 ± 15	355 ± 10	34.2 ± 2.6
ECAP	518 ± 5	524 ± 8	14.6 ± 1.1
quenching + aging at 500°C for 2 h	257 ± 6	391 ± 9	32.6 ± 2.5
ECAP + aging at 500°C for 2 h	379 ± 26	446 ± 21	21.0 ± 2.2

24 nm is noted. It should be also noted the presence of coarse chromium-phase particles 370 ± 18 nm in average size, which have the regular oval shape (Fig. 3e).

The Cu–10% Fe alloy subjected to ECAP and aging mainly is characterized by the band-type microstructure (Figs. 3c, 3d). In this case, both high-angle boundaries of fragments and low-angle boundaries consisting of dislocation walls are found. The average lateral size of fragments is 220 ± 9 nm. Moreover, the existence of grains and subgrains with an average size of 357 ± 27 nm is found. Iron-phase particles with an average size of 13 ± 1 nm are arranged mainly within the grain body; they also can be observed along dislocations within dislocation networks (Fig. 3f). It should also be noted the existence of extinction contours along boundaries of some grains, which indicate the relaxation processes of stresses accumulated at boundaries.

Table 2 gives results of mechanical tests of the Cu–7% Cr and Cu–10% Fe alloys subjected to quenching, ECAP, and aging. It follows from these data that, as a result of significant refining the microstructure of both the ECAP-processed alloys, they are substantially strengthened; however, the plasticity decreases simultaneously. The ultimate tensile strength of the Cu–7% Cr alloy increases from 288 ± 6 MPa (corresponding to the quenched state) to 480 ± 6 MPa (observed after ECAP); in this case, the plasticity decreases from 48.0 ± 4.3 to 14.8 ± 1.3%, respectively. The ultimate tensile strength of the Cu–10% Fe alloy increases from 355 ± 10 MPa (corresponding to the quenched state) to 524 ± 8 MPa (observed after ECAP); in this case, the plasticity decreases from 34.2 ± 2.6 to 14.6 ± 1.1%, respectively.

The subsequent aging under optimum conditions leads to changing both the strength and plastic characteristics (see Table 2). During aging of the quenched Cu–7% Cr alloy, the increase in its ultimate strength to 430 ± 27 MPa is observed; the plasticity decreases to 21.2 ± 4.9%. The ultimate strength of the quenched Cu–10% Fe alloy slightly increases after aging to 391 ± 9 MPa; however, the plasticity remains close to that of the quenched alloy (32.6 ± 2.5%). Such a behavior of the alloys after quenching is due to the copper-based supersaturated solid solution decomposition and precipitation of fine chromium and iron particles. On the contrary, the aging of deformed alloys does not lead to the increase in their strength but slightly increases their plasticity. The ultimate strength of the ECAP-processed Cu–7% Cr alloy is unchanged after aging at 425°C relatively to the strength of the initially deformed state and is 472 ± 12 MPa; at the same time, the plasticity increases to 18.1 ± 3.6%. The deformed Cu–10% Fe alloy subjected to aging at 500°C exhibits the decrease in the ultimate strength to

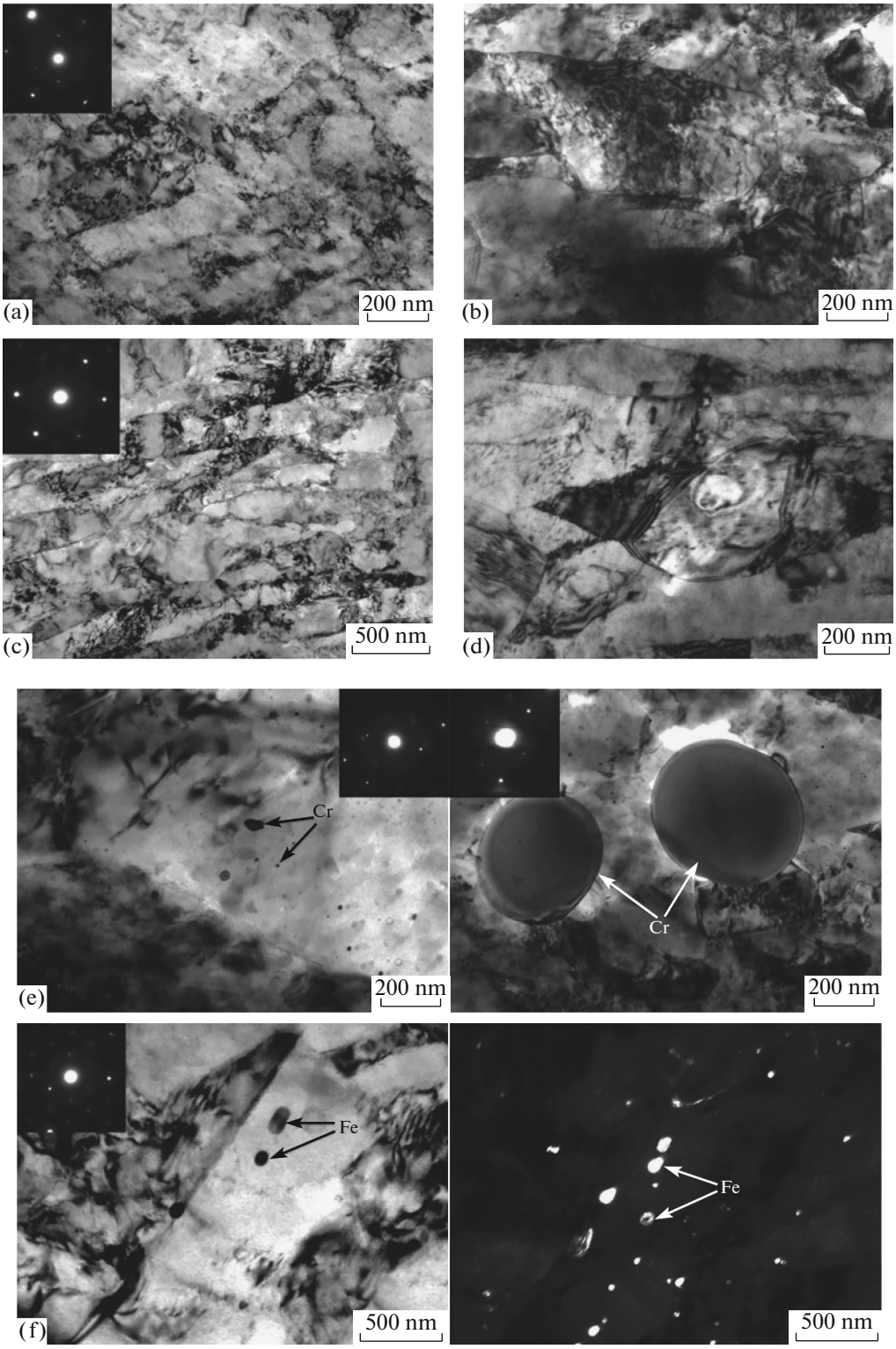

Fig. 3. Microstructure of (a, b) Cu–7% Cr and (c, d) Cu–10% Fe alloys subjected to ECAP and subsequent aging and (e) chromium and (f) iron phase particles precipitated in the alloys after aging.

446 ± 21% and simultaneous increase in the plasticity to 21.0 ± 2.2%.

The change in the strength after aging can be due to the simultaneous effect of two factors; these are the grain growth caused by heating and the solid solution decomposition. In this case, the first factor should lead to a decrease in the strength, whereas the second factor leads to its increase. In our case, two versions of

developments are observed. In the case of the Cu–7% Cr alloy, both the occurred processes affect the strength; however, the effects have opposite signs. Because of this, after aging, neither increase nor decrease in the strength is observed. The grains growth in the Cu–10% Fe alloy is likely to play the predominant role over the precipitation strengthening, which, in the end, leads to the decrease in the strength. However, in this case, the solid solution decomposition and grain growth positively affect the plasticity of both alloys.

When summarizing the data, we can conclude that ECAP is the advanced method for the treatment of the Cu–7% Cr and Cu–10% Fe alloys. The use of quenching, ECAP, and subsequent aging allows us to obtain, for the Cu–7% Cr alloy, the combination of the high electrical conductivity (~81% IACS) and strength (~470 MPa) at the sufficiently high level of plasticity (~18%). The electrical conductivity, strength, and plasticity of the Cu–10% Fe alloy are ~50% IACS, ~450 MPa, and ~21%, respectively. It should be noted that the values of the electrical conductivity of the Cu–7% Cr alloy are substantially higher than those for the Cu–10% Fe alloy; this fact makes the Cu–7% Cr alloy more promising for the application in electrical industry.

CONCLUSIONS

(1) ECAP leads to the formation of an UFG mixed structure. For both alloys, the formation of shear bands ~100 nm wide is observed. Moreover, the formation of a grain–subgrain structure with an average size of structural components of 250 ± 13 and 155 ± 7 nm in the Cu–7% Cr and Cu–10% Fe alloys, respectively.

(2) Aging of the quenched Cu–7% Cr and Cu–10% Fe alloys was found to lead to a simultaneous increase in the microhardness and the electrical conductivity. At the same time, aging of the ECAP-processed alloys leads to the decomposition of a copper-based supersaturated solid solution, which favors an increase in their electrical conductivity but negatively affects the microhardness of the alloys.

(3) Aging of the ECAP-processed alloys leads to an increase in the average size of structural components. In particular, shear bands 130 ± 7 nm wide and grains and subgrains with an average size of 317 ± 24 nm are present in the Cu–7% Cr alloy after aging. The structure of the Cu–10% Fe alloy subjected to ECAP and aging consists of shear bands 220 ± 9 nm wide and grains and subgrains 357 ± 27 nm in average size. In this case, the Cu–7% Cr alloy is characterized by the presence of fine and coarse chromium phase particles 5–12 and ~370 nm in size, respectively. The presence of iron-phase particles ~13 nm in size was found in the Cu–10% Fe alloy.

(4) The formation of an UFG structure leads to a substantial increase in the strength of both alloys and a simultaneous decrease in their plasticity. The subsequent aging increases the strength of the quenched alloys and simultaneously decreases their plasticity. At the same time, aging does not affect the strength of the deformed Cu–7% Cr alloy but leads to softening the of deformed Cu–10% Fe alloy. Aging of both ECAP-processed alloys leads to an increase in their plasticity.

(5) The best combination of the strength (~470 MPa), the plasticity (~18%), and the electrical conductivity (~81% IACS) was reached for the Cu–7% Cr alloy subjected to quenching, ECAP, and subsequent aging at 425°C for 2 h.

FUNDING

This work was performed in terms of state assignment no. 075-00328-21-00.

REFERENCES

1. I. P. Semenova, J. M. Modina, A. V. Polyakov, G. V. Klevtsov, N. A. Klevtsova, I. N. Pigaleva, R. Z. Valiev, and T. G. Langdon, "Fracture toughness at cryogenic temperatures of ultrafine-grained Ti–6Al–4V alloy processed by ECAP," Mater. Sci. Eng. A **716**, 260–267 (2018).
2. E. D. Merson, P. N. Myagkikh, G. V. Klevtsov, D. L. Merson, and A. Yu. Vinogradov, "Effect of equal-channel angular pressing and current density of cathode hydrogenation on the hydrogen capture in low-carbon steel," Pis'ma Mater. **10** (2), 152–157 (2020).
3. Y. Estrin, N. Martynenko, N. Anisimova, D. Temralieva, M. Kiselevskiy, V. Serebryany, G. Raab, B. Straumal, B. Wiese, R. Willumeit-Römer, and S. Dobatkin, "The effect of equal-channel angular pressing on the microstructure, the mechanical and corrosion properties and the anti-tumor activity of magnesium alloyed with silver," Mater. **12** (23), 3832 (2019).
4. S. V. Dobatkin, O. V. Rybal'chenko, and G. I. Raab, "Formation of a submicrocrystalline structure in austenitic 08Kh18N10T steel during equal-channel angular pressing followed by heating," Russ. Metall. (Metally), No. 1, 42–48 (2006).
5. N. Martynenko, E. Lukyanova, N. Anisimova, M. Kiselevskiy, V. Serebryany, N. Yurchenko, G. Raab, N. Birbilis, G. Salishchev, S. Dobatkin, and Y. Estrin, "Improving the property profile of a bioresorbable Mg–Y–Nd–Zr alloy by deformation treatments," Materialia **13**, 100841 (2020).
6. S. V. Dobatkin, W. Skrotzki, O. V. Rybalchenko, V. F. Terent'ev, A. N. Belyakov, D. V. Prosvirnin, G. I. Raab, and E. V. Zolotarev, "Structural changes in metastable austenitic steel during equal channel angular pressing and subsequent cyclic deformation," Mater. Sci. Eng. A **723**, 141–147 (2018).
7. W. Wang, Q. Pan, X. Wan, Y. Sun, L. Long, and Z. Huang, "Mechanical properties and microstructure evolution of ultra-high strength Al–Zn–Mg–Cu alloy

processed by room temperature ECAP with post aging," Mater. Sci. Eng. A **731**, 195–208 (2018).

8. T. Tański, P. Snopiński, K. Prusik, and M. Sroka, "The effects of room temperature ECAP and subsequent aging on the structure and properties of the Al–3%Mg aluminium alloy," Mater. Charact. **133**, 18–195 (2017).
9. G. Purcek, H. Yanar, M. Demirtas, Y. Alemdag, D. V. Shangina, S. V. Dobatkin, "Optimization of strength, ductility and electrical conductivity of Cu–Cr–Zr alloy by combining multi-route ECAP and aging," Mater. Sci. Eng. A **649**, 114–122 (2016).
10. N. Liang, J. Liu, S. Lin, Y. Wang, J. T. Wang, Y. Zhao, and Y. Zhu, "A multiscale architectured CuCrZr alloy with high strength, electrical conductivity and thermal stability," J. Alloys Compd. **735**, 1389–1394 (2018).
11. Y. X. Ye, X. Y. Yang, J. Wang, X. K. Zhang, Z. L. Zhang, and T. Sakai, "Enhanced strength and electrical conductivity of Cu–Zr–B alloy by double deformation-aging process," J. Alloys Compd. **615**, 249–254 (2014).
12. X. L. Guo, Z. Xiao, W. T. Qiu, Z. Li, Z. Q. Zhao, X. Wang, and Y. Jiang, "Microstructure and properties of Cu–Cr–Nb alloy with high strength, high electrical conductivity and good softening resistance performance at elevated temperature," Mater. Sci. Eng. A **749**, 281–290 (2019).
13. S. Uchida, T. Kimura, T. Nakamoto, T. Ozaki, T. Miki, M. Takemura, Y. Oka, and R. Tsubota, "Microstructures and electrical and mechanical properties of Cu–Cr alloys fabricated by selective laser melting," Mater. Design **175**, 107815 (2019).
14. R. B. Naik, K. V. Reddy, G. M. Reddy, and R. A. Kumar, "Microstructure, mechanical and wear properties of friction stir processed Cu–1.0%Cr alloys," Fusion Eng. Design **164**, 112202 (2021).
15. S. V. Dobatkin, J. Gubicza, D. V. Shangina, N. R. Bochvar, and N. Y. Tabachkova, "High strength and good electrical conductivity in Cu–Cr alloys processed by severe plastic deformation," Lett. Mater. **153**, 5–9 (2015).
16. K. Liu, Z. Jiang, J. Zhao, J. Zou, Z. Chen, and D. Lu, "Effect of directional solidification rate on the microstructure and properties of deformation-processed Cu–7Cr–0.1Ag in situ composites," J. Alloys Compd. **612**, 221–226 (2014).
17. J. Deng, X. Zhang, S. Shang, F. Liu, Z. Zhao, and Y. Ye, "Effect of Zr addition on the microstructure and properties of Cu–10Cr in situ composites," Mater. Design **30** (10, 4444–4449 (2009).
18. J. S. Song, H. S. Kim, C. T. Lee, and S. I. Hong, "Deformation processing and mechanical properties of Cu–Cr–X (X = Ag or Co) microcomposites," J. Mater. Proc. Technol. **130–131**, 272–277 (2002).
19. M. Wang, R. Zhang, Z. Xiao, S. Gong, Y. Jiang, and Z. Li, "Microstructure and properties of Cu–10 wt % Fe alloy produced by double melt mixed casting and multi-stage thermomechanical treatment," J. Alloys Compd. **820**, 153323 (2020).
20. S. Liu, J. Jie, Z. Guo, S. Yue, and T. Li, "A comprehensive investigation on microstructure and magnetic properties of immiscible Cu–Fe alloys with variation of Fe content," Mater. Chem. Phys. **238**, 21909 (2019).
21. M. Wang, Y. Jiang, Z. Li, Z. Xiao, S. Gong, W. Qiu, and Q. Lei, "Microstructure evolution and deformation behaviour of Cu–10 wt % Fe alloy during cold rolling," Mater. Sci. Eng. A **801**, 140379 (2021).
22. A. Lukyanov, A. Churakova, A. Filatov, E. Levin, R. Valiev, D. Gunderov, and E. Antipov, "Microstructure refinement in Cu–Fe alloy using high pressure torsion," IOP Conf. Ser.: Mater. Sci. Eng. **63**, 012102 (2014).
23. *Phase Diagrams of Binary Metallic System: Handbook*, Ed. by N. P. Lyakishev (Mashinostroenie, Moscow, 1997), Vol. 2.
24. E. A. Lukyanova, N. S. Martynenko, V. N. Serebryany, A. N. Belyakov, L. L. Rokhlin, S. V. Dobatkin, and Y. Z. Estrin, "Structure and mechanical and corrosion properties of a magnesium Mg–Y–Nd–Zr alloy after high pressure torsion," Russ. Metall. (Metally), No. 6, 912–921 (2017).
25. I. A. Faizov, G. I. Raab, S. N. Faizova, N. G. Zaripov, and D. A. Aksenov, "The role of phase transitions in the evolution of dispersion particles in chromium bronzes upon the equal channel angular pressing," Lett. Mater. **6** (2), 132–137 (2016).
26. D. A. Aksenov, R. Asfandiyarov, G. I. Raab, and G. B. Isyandavletova, "Features of the physico-mechanical behavior of UFG low-alloyed bronze Cu–1Cr–0.08Zr produced by severe plastic deformation," IOP Conf. Ser.: Mater. Sci. Eng. **179**, Conf.1. (2017). https://doi.org/10.1088/1757-899X/179/1/012001

Translated by N. Kolchugina